Int. J. Heat Mass Transfer. Vol. 35, No. 6, pp. 1507–1518, 1992
Printed in Great Britain

0017–9310/92 $5.00 + 0.00

Buoyancy-driven flow in an enclosure with time periodic boundary conditions

M. KAZMIERCZAK
Department of Mechanical, Industrial, and Nuclear Engineering, University of Cincinnati, Mail Location 72, Cincinnati, OH 45221-0072, U.S.A.

and

Z. CHINODA
Pro-Quip Inc., 850 E. Highland, Macedonia, OH 44056, U.S.A.

(*Received* 3 *January* 1991 *and in final form* 14 *May* 1991)

Abstract—The problem of laminar buoyancy-driven flow in a square cavity driven by a warm vertical wall, having a uniform surface temperature whose magnitude is changing periodically with time, is investigated numerically. The warm wall surface temperature varies sinusoidally, oscillating about a fixed mean temperature. The opposite cold wall is maintained at a constant temperature. Solutions are obtained for a number of different cases which illustrate the effects of the oscillating surface temperature on the fluid flow and the heat transfer through the enclosure. The transient solutions obtained are all periodic in time. The streamlines show that a weak secondary flow cell intermittently appears and then disappears in the upper corner of the enclosure near the hot driving wall, rotating in a direction opposite to the main flow. The instantaneous heat flux through the hot wall fluctuates greatly in time and over certain times heat removal occurs over a large segment of the hot driving surface. The effect of the periodically changing wall temperature is felt only partially into the enclosure and, overall, the time-averaged heat transfer across the enclosure is rather insensitive to the time-dependent boundary condition.

INTRODUCTION

NUMEROUS studies exist in the literature that investigate natural convection in enclosures. Interest is justified by its many applications which include heating and cooling of buildings, solar energy utilization, thermal energy storage, convection in lakes and small bodies of water, and more recently, cooling of electronic equipment. An overview of this important area in heat transfer is given in ref. [1].

The majority of the published work in free convection in enclosures that exists today considers the steady-state phenomenon. The driving walls of the enclosure are customarily held at a constant temperature or heat flux. However, in many of the applications listed above, the thermal boundary conditions vary with time and, therefore, in reality, a transient or unsteady convective flow ensues. More specifically, in the cooling of electronic equipment, the electrical components are frequently energized intermittently and, therefore, generate heat in an unsteady manner. This heat is then removed by natural convection. Time-dependent boundary conditions are also clearly present in building heat transfer where the 'unsteadiness' is induced by the changing ambient conditions and by intermittent usage of the heating system. In spite of these facts, little work has been performed in the field of transient natural convection in enclosures.

The limited number of transient studies almost unanimously considered a *step change* (with respect to time) in the wall boundary conditions [2–8]. In these studies, the researchers examined the changing temperature and flow fields as they evolved over time as the system approached the new steady-state solution. The case of a vertical fluid layer initially motionless and at a uniform temperature when subjected to a sudden change in the two end wall temperatures to $T \pm \Delta T$, respectively, at time $t = 0$ was investigated in refs. [2–6]. The transient behavior of an enclosure when the temperature of only a single wall was suddenly changed, while the other walls were adiabatic, was studied by Nicolette *et al.* [7] and Hall *et al.* [8].

Transient natural convection studies involving more physically realistic boundary conditions where the wall temperature gradually changes over time have received less attention. To the best of the authors' knowledge, the only available studies of this type, pertaining to rectangular geometry, are the works of Schladow *et al.* [5] and Vasseur and Robillard [9]. The former study mainly investigated transient natural convective flow induced by a sudden change in wall temperature. In an attempt to explain discrepancies found between their numerical simulation and experimental observations of the flow field, Schladow *et al.* performed an additional run in which they ramped the driving wall temperature in a linear fashion over a five second interval equal in magnitude to the step change. Comparison between the two simulations

NOMENCLATURE

a	dimensionless amplitude
A	amplitude
c_p	specific heat at constant pressure
f	frequency
g	gravitational acceleration
H	vertical height of the system
h	dimensionless height
k	thermal conductivity
L	horizontal length of the system
m	number of horizontal grid lines
n	number of vertical grid lines
Nu	Nusselt number, equation (9)
p	dimensionless time period
P	time period, $1/f$
Pr	Prandtl number, ν/α
q	heat transfer rate per unit area
Ra	thermal Rayleigh number, $g\beta(\bar{T}_h - T_c)H^3/\alpha\nu$
t	time
T	temperature
u	dimensionless horizontal velocity component
U	horizontal velocity component
v	dimensionless vertical velocity component
V	vertical velocity component
x	dimensionless horizontal Cartesian coordinate
X	horizontal Cartesian coordinate
y	dimensionless vertical Cartesian coordinate
Y	vertical Cartesian coordinate
Z	dummy variable.

Greek symbols

α	thermal diffusivity, $k/\rho c_p$
β	coefficient of thermal expansion
γ	relaxation parameter
θ	dimensionless temperature
λ	prescribed error
μ	viscosity
ν	kinematic viscosity, μ/ρ
ρ	fluid density
τ	dimensionless time
ψ	dimensionless stream function
ω	dimensionless vorticity.

Subscripts

c	cold wall
h	hot wall
i, j	nodal location
max	maximum.

Superscripts

r	iteration number
$\bar{}$	denoting a quantity averaged over time.

revealed that the changing wall temperature had negligible effect on the predicted flow and temperature fields. Vasseur and Robillard [9] investigated the case of transient convective cooling of a rectangular enclosure with end walls that continually decreased in temperature at a constant rate. After a sufficiently long time, the solution became quasi-steady, and the flow velocities, flow pattern, and the temperature difference between the fluid and the wall became constant with time. An interesting flow pattern developed for the high Rayleigh number case which consisted of a primary set of counter-rotating cells with an additional second set of counter-rotating vortices located near the top wall at the centerline of the enclosure.

This paper investigates buoyancy-driven flow in a differentially heated vertical enclosure driven by a warm wall with a periodically changing surface temperature. The hot wall temperature varies sinusoidally about a mean value, and the cold wall is maintained at a fixed temperature. The cyclic variation of the hot driving wall approximates the boundary condition found in many solar and energy storage applications, building heat transfer, and many environmental processes. Also, it is common to many industrial set-ups as a result of the operation of the control system. Lastly, time variation in surface temperature occurs in electronic devices as a consequence of periodically switching the current on and off in the various electrical components.

The main objective of the present paper is to determine the effect of the oscillating surface temperature on the fluid flow and heat transfer within the cavity. More specifically, the effect of the amplitude and the period of the surface temperature oscillation on the temperature and flow fields and on the instantaneous and time-averaged Nusselt numbers will be documented.

MATHEMATICAL FORMULATION

A schematic representation of the system under investigation is shown in Fig. 1. The top and bottom horizontal walls are adiabatic, and the right side wall is maintained at a constant cold temperature. The temperature of the opposing hot vertical driving wall varies sinusoidally with time about a mean value, $\bar{T}_h$, with amplitude A and frequency f. The hot wall temperature is greater than the cold wall temperature at all times, as graphically depicted in Fig. 2. Given the oscillatory boundary condition, it is clear that the

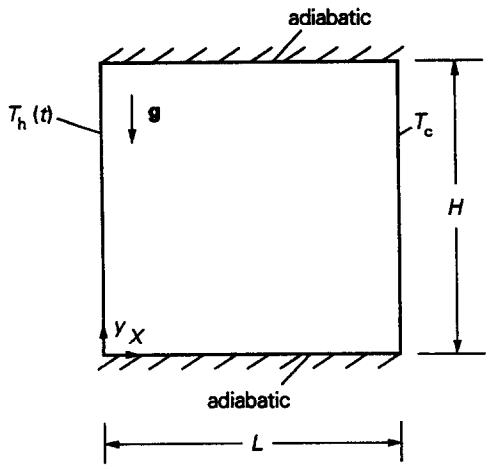

FIG. 1. System of interest.

solution to the system becomes periodic in time after a sufficient number of cycles have past. Thus, this problem has two distinct transient time periods; first, the initial transient from $t = 0$ to the time when the solution starts repeating itself, and second, the steady-period solution itself. Of greater interest is the latter period where the effects of the amplitude and the frequency of the hot wall oscillation are better discerned. It is the periodic solution that is the focus of our investigation.

To determine the behavior of the system described above we solve numerically the pertinent governing equations. The flow in this analysis is laminar and two-dimensional. The thermophysical properties of the fluid are treated as constant everywhere except for the density in the buoyancy force term in the momentum equations. There, according to the Boussinesq approximation, the density is assumed to be a linear function of temperature. To aid in the numerical solution of the governing equations we first introduce the dimensionless stream function, ψ, and dimensionless vorticity, ω, into the two momentum equations, eliminate the pressure gradient terms and obtain a single vorticity equation. With the foregoing comments in mind, the dimensionless stream function/vorticity formulations of the governing equations are:

$$\partial\omega/\partial\tau + u(\partial\omega/\partial x) + v(\partial\omega/\partial y) = Pr\nabla^2\omega + Ra\,Pr(\partial\theta/\partial x) \quad (1)$$

$$\partial\theta/\partial\tau + u(\partial\theta/\partial x) + v(\partial\theta/\partial y) = \nabla^2\theta \quad (2)$$

where

$$u = \partial\psi/\partial y; \quad v = -\partial\psi/\partial x; \quad \omega = -\nabla^2\psi. \quad (3)$$

The boundary conditions for the problem of interest read:

$$u = v = \psi = 0;$$

$$\partial\theta/\partial y = 0 \quad \text{at} \quad y = 0, 1 \quad \text{and} \quad 0 \leqslant x \leqslant L/H \quad (4)$$

$$u = v = \psi = 0;$$

$$\theta = 0 \quad \text{at} \quad x = L/H \quad \text{and} \quad 0 \leqslant y \leqslant 1 \quad (5)$$

$$u = v = \psi = 0;$$

$$\theta = 1 + a\sin(2\pi\tau/p) \quad \text{at} \quad x = 0 \quad \text{and} \quad 0 \leqslant y \leqslant 1. \quad (6)$$

All symbols have been defined in the Nomenclature. The non-dimensionalization was carried out using the following dimensionless variables:

$$x = X/H; \quad y = Y/H; \quad u = U/(\alpha/H);$$
$$v = V/(\alpha/H);$$
$$\theta = (T - T_c)/(\bar{T}_h - T_c); \quad \tau = t/(H^2/\alpha);$$
$$p = P/(H^2/\alpha); \quad a = A/(\bar{T}_h - T_c). \quad (7)$$

The dimensionless parameters that appear in the problem include: the thermal Rayleigh number, Ra, and the Prandtl number, Pr, the dimensionless amplitude, a, and the dimensionless period, p, of oscillating warm wall. It is the effect of these last two parameters on the flow and heat transfer phenomena within the system that is the main focus of our investigation.

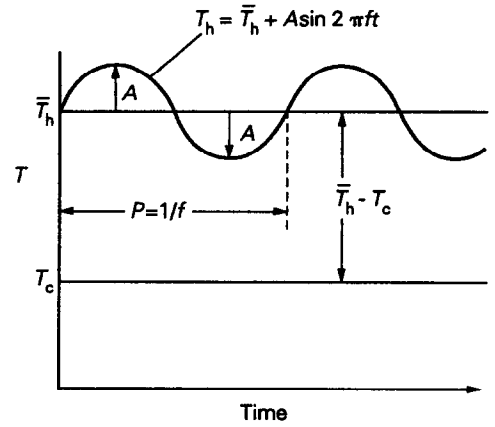

FIG. 2. The hot wall time-dependent boundary condition.

NUMERICAL SOLUTION

The finite difference method was used to solve the system of equations specified in the previous section. The dimensionless governing equations (1)–(3) were discretized using the control volume formulation and the power law scheme [10] was employed to calculate the heat and mass fluxes across the boundaries of each control volume. The algebraic equations were then solved iteratively using the Gauss–Seidel method subject to the discretized boundary conditions, equations (4)–(6). In addition, the vorticity at the walls of the enclosure must be specified and the formulation given by Thom [11] was used.

Convergence was achieved at each time step according to the following criterion:

$$\frac{\sum_{i,j} |Z_{i,j}^{r+1} - Z_{i,j}^{r}|}{\sum_{i,j} |Z_{i,j}^{r+1}|} < \lambda \tag{8}$$

where Z stands for ω, ψ, or T, r is the iteration level and λ is a prescribed error ($\lambda = 10^{-5}$). Relaxation was used to aid the convergence in solving the vorticity equation ($\gamma = 0.4$), although it was not needed in the solution of the energy or the stream function equations.

Time was advanced from one time step to the next starting from the converged solution of the previous time step. The process continued until the solution to the problem became periodic due to the cyclic nature of the boundary condition. To model accurately the changing hot wall temperature, a single oscillation was subdivided into 1000 time steps. To minimize the number of cycles that are necessary for the solution to become periodic (i.e. the initial transient to die), we began all the simulations reported in this paper starting from an initial temperature and flow field; in fact, the steady-state solution to the same problem without temperature oscillation ($a = 0$) of the hot wall. Proceeding in this manner, we found the solution soon began repeating itself, often in as few as two cycles. Note that this method resulted in enormous savings of computational time as compared to the situation of starting the simulation from a motionless and isothermal condition.

A non-uniform grid ($m = 36$ by $n = 45$), shown in Fig. 3, was used in all of the simulations. The mesh is finer at the walls where sharp temperature gradients are expected. The code was checked for accuracy against the earlier published numerical results of Patterson and Imberger [2] for the problem of transient buoyancy-induced flow in a square cavity with a time step change in wall temperature for $Ra = 1.4 \times 10^5$ and $Pr = 7$. Suddenly, one vertical wall became hot, and the opposite wall was cooled while the two horizontal walls were adiabatic. We found the streamlines and isotherm patterns obtained using our code to be practically identical to the published finding reported in ref. [2] over all times during the transient evolution of the problem. A detailed comparison is not shown for brevity but is found in ref. [12]. In the final steady-state, our Nusselt number differed by only 0.21% when similar grids were used.

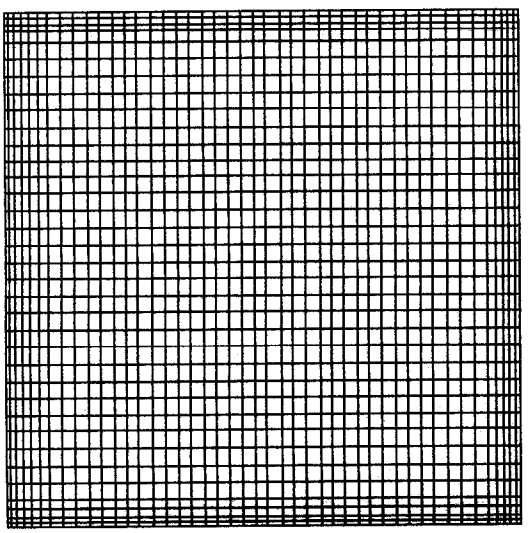

FIG. 3. Computational mesh.

RESULTS AND DISCUSSION

A total of five numerical experiments were performed. The values of the parameters used for each of these runs are summarized in Table 1. The thermal Rayleigh number, the Prandtl number, and the aspect ratio of the enclosure were all held fixed throughout this study in order to focus our attention on the parameters that directly pertain to the oscillatory boundary condition. The dimensionless period was fixed at $p = 0.01$ for the first three simulations and the dimensionless amplitude of the hot wall varied, set at 0.4, 0.2, and 0.8, respectively. In the last two runs the amplitude was constant ($a = 0.4$), and the dimensionless period of the oscillating hot wall changed. It was first halved (simulation 4) and then it was doubled (simulation 5) with respect to the period used in the earlier simulations.

Figures 4–7 report the main results of the first simulation. The dimensionless hot wall boundary condition driving the flow is graphically represented by Fig. 4. The amplitude of the hot wall variation was 0.4, and its period was 0.01. The simulation was carried out for a total of four cycles, and it was found that under these conditions the solution became periodic after just two cycles (i.e. the results of the fourth cycle were identical to the results of the third cycle).

The sequence of streamlines and isotherms, plotted at eight different times over the duration of the fourth cycle, is shown in Fig. 5. Time increases from Fig. 5(a) to Fig. 5(h) in equal increments (1/8 cycle), and corresponds to the times indicated by the dashed lines drawn on the fourth cycle of the last figure. It should be made clear that this sequence repeats itself, and the very next streamline and isotherm patterns generated following Fig. 5(h) are identical to Fig. 5(a).

The streamline plots of Fig. 5 show that the flow field is dominated by a primary large cell filling most of the cavity rotating in a clockwise direction. Positioned in the upper left hand corner of the enclosure, a weak small secondary cell exists rotating in the counterclockwise direction. The secondary cell initially appears at $\tau = 0.035$ (Fig. 5(e)), the time at which the hot wall temperature equals the average hot wall temperature, $\bar{T}_h$, after decreasing from the maximum value. The secondary cell grows in size and intensity (Figs. 5(e)–(h)) over the second half of the time period of the hot wall temperature variation where the instantaneous hot wall temperature is

Table 1. Summary of numerical simulations

Simulation number	Ra	Pr	a	p	$\Delta\tau$	τ_{final}	L/H	Grid $(m\times n)$
1	1.4×10^5	7	0.4	0.01	1×10^{-5}	0.04	1	36×46
2	1.4×10^5	7	0.2	0.01	1×10^{-5}	0.04	1	36×46
3	1.4×10^5	7	0.8	0.01	1×10^{-5}	0.04	1	36×46
4	1.4×10^5	7	0.4	0.005	1×10^{-5}	0.02	1	36×46
5	1.4×10^5	7	0.4	0.02	1×10^{-5}	0.08	1	36×46

always less than the average value (Fig. 4). Continuing further in time, the region of secondary recirculation decreases greatly in size (Fig. 5(a)) as the hot wall temperature increases and equals $\bar{T}_h$. The secondary cell then totally disappears as T_h increases above $\bar{T}_h$ (Fig. 5(b)).

The flow in the main cell is also time-dependent. It contains a core region at the center and, at the walls, regions of boundary layer type flow typical of natural convection enclosure flows at high Ra. The magnitude and the location of the maximum stream function change with time according to the changing hot wall temperature. During the first half or 'warm' portion of the cycle when $T_h > \bar{T}_h$ (Figs. 5(b)–(e)), the maximum stream function, ψ_{max}, in the main cell has the largest value ($\psi_{max} = 17$ at $\tau = 0.03375$), and is positioned toward the hot wall side of the enclosure. During the second half of the cycle, simultaneous with the appearance of the secondary flow, the flow intensity in the main cell is much weaker ($\psi_{max} = 11$ at $\tau = 0.03875$), and its location has shifted toward the vertical cold wall. Comparing the time the maximum stream function is greatest to the time at which the hot wall temperature is maximum reveals that there exists a *phase shift* in which ψ_{max} lags the hot wall temperature. This delay is attributed to the time required for the heat transfer to occur, as well as the time required for the buoyancy force to overcome the inertia and viscous forces of the system.

The isotherms plotted in Fig. 5 also reveal interesting system behavior. During the time when the hot wall temperature is increasing (Figs. 5(a)–(c)), a well defined thermal boundary layer is visible on both vertical walls. However, when the hot wall temperature decreases the thermal boundary layer on the hot wall begins to break down (Figs. 5(d)–(f)). The fluid near the hot wall, heated earlier to a higher temperature, now 'floats' to the top of the enclosure and forms a warm pocket (Figs. 5(g), (h)). This pocket contains fluid warmer than the hot wall. The hot wall at this time drives the flow in the secondary recirculation cell in the counterclockwise direction (*down* the hot wall). The warm region near the top of the enclosure disappears during the next cycle (Figs. 5(h)–(b)) as energy diffuses and is advected outward until finally achieving the rising hot wall temperature.

Note that over the time period when a portion of the fluid in the cavity is actually warmer than the hot wall temperature, heat is removed from the system through the hot wall. For example, the isotherms in Fig. 5(g) show that energy enters the enclosure only in the bottom half of the hot wall while energy *leaves* through the top half of the hot wall. Recall that this happens in spite of the fact that the hot wall is, at all times, at a higher temperature than the cold wall. It is important to point out that this behavior could not have been predicted if a quasi-steady approach was used in solving the problem.

A Nusselt number versus time plot (Fig. 6) also clearly shows back heat flow. The Nusselt number is plotted over all four cycles of the numerical simulation and is evaluated at three different locations: the hot wall ($x = 0$), the cold wall ($x = L/H$), and at a position midway ($x = (L/2)/H$) between the two vertical walls. The Nusselt number is defined as

$$Nu = q/kH(\bar{T}_h - T_c)/L = L/H\int_0^1 (u\theta - \partial\theta/\partial x)\Big|_{x=} dy \tag{9}$$

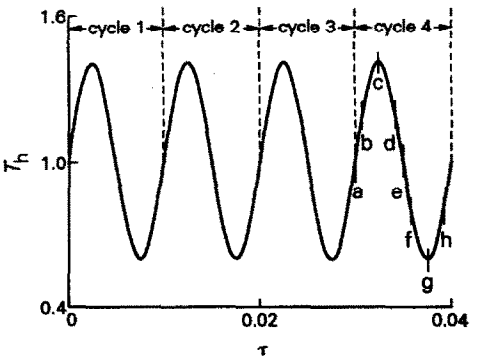

FIG. 4. Dimensionless oscillatory boundary condition for simulation 1.

the ratio of the actual heat transfer across the enclosure compared to that by pure conduction heat transfer (based on the time-averaged hot wall temperature $\bar{T}_h$). Note that θ in the definition of the Nusselt number is the instantaneous dimensionless temperature. It is clear from Fig. 6 that the Nusselt number cycles in a similar manner to the hot wall temperature. The value of the Nusselt number at the hot wall fluctuates the most, from a maximum periodic value of $Nu_h = 14.67$ at $\tau = 0.0314$ to a minimum value of $Nu_h = -3.97$ at $\tau = 0.0364$. The hot wall Nusselt number is negative over a short duration of the cycle ($0.0349 \leqslant \tau \leqslant 0.0378$), stating that over this time period there is

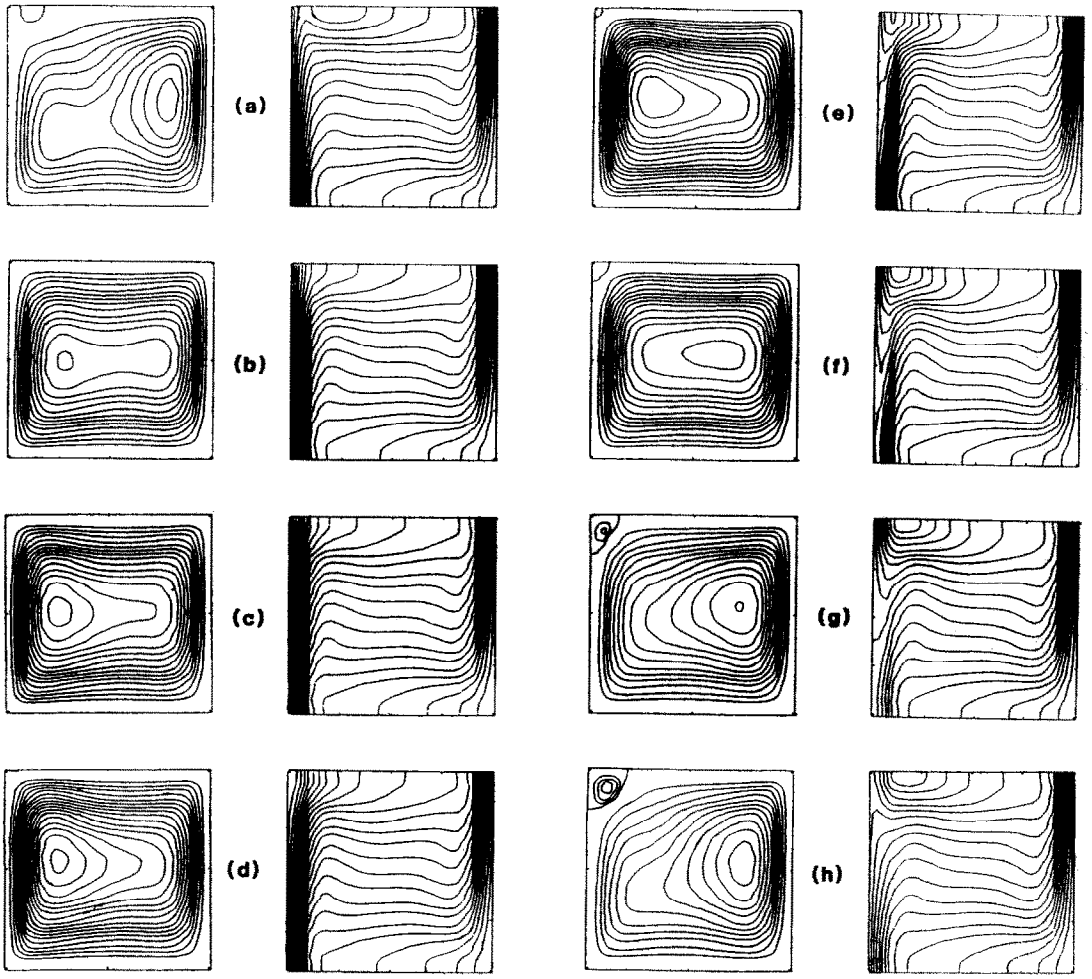

FIG. 5. Periodic streamlines (first and third columns) and isotherms (second and fourth columns) for simulation 1. (a) $\tau = 0.03$, $\psi_{max} = 10$. (b) $\tau = 0.03125$, $\psi_{max} = 13$. (c) $\tau = 0.0325$, $\psi_{max} = 15$. (d) $\tau = 0.3375$, $\psi_{max} = 17$. (e) $\tau = 0.0350$, $\psi_{max} = 16$. (f) $\tau = 0.03625$, $\psi_{max} = 14$. (g) $\tau = 0.03750$, $\psi_{max} = 13$. (h) $\tau = 0.03875$, $\psi_{max} = 11$. Streamlines increment $\Delta\psi = 1.0$ for primary cell and $\Delta\psi = -0.1$ for secondary cell. Isotherms increment $\Delta\theta = 0.05$ starting at $\theta = 0$ from the right.

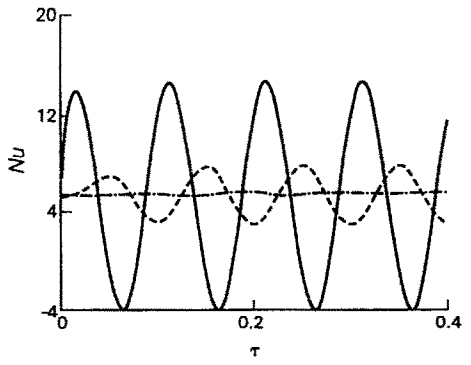

FIG. 6. Nusselt number dependence on time for simulation 1. Hot wall, $x = 0$ (——); cold wall, $x = L/H$ (— · —); midpoint, $x = (L/2)/H$ (– – –).

an overall energy loss or a *net* heat transfer exiting the cavity through the hot wall.

Midway through the enclosure, $x = (L/2)/H$, the Nusselt number also varies periodically in time but changes much less in magnitude and has a phase lag compared to the hot wall Nusselt number. It takes on only positive values, indicating that the net heat flow is always toward the direction of the cold wall. At the cold wall ($x = L/H$), the Nusselt number is almost constant with respect to time and only a very slight modulation is visible. Thus, for most practical engineering applications, the cold wall heat transfer is essentially constant.

The temperature and velocity profiles (Fig. 7) explain why the heat transfer variation with time decreases from the hot wall to the cold wall. Hori-

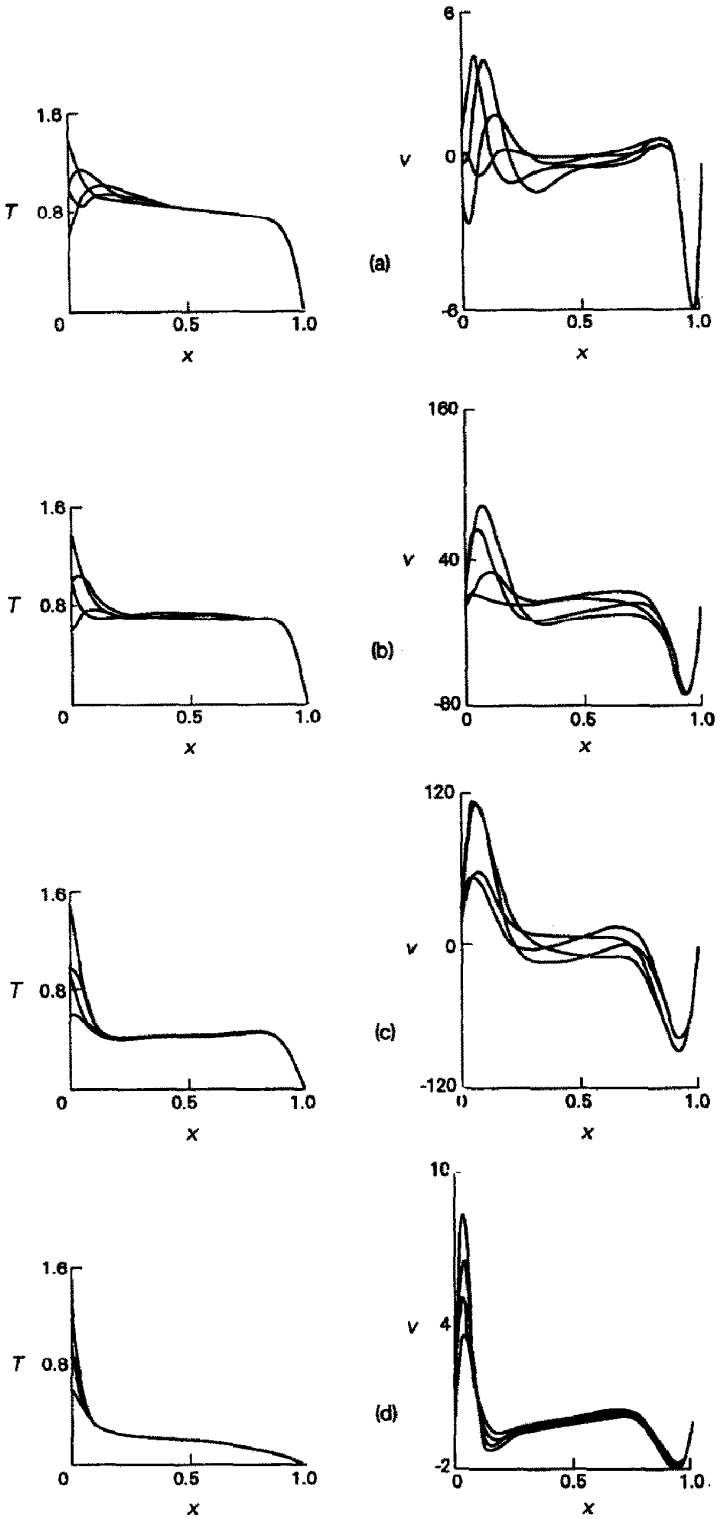

FIG. 7. Simulation 1 periodic temperature profiles (left column) and vertical velocity component profiles (right column) at quarterly time increments for selected heights. (a) $y = 0.93$. (b) $y = 0.80$. (c) $y = 0.40$. (d) $y = 0.07$.

zontal temperature and velocity profiles at four different enclosure heights, $y = 0.93$, 0.80, 0.40, and 0.07, are shown in Figs. 7(a)–(d), respectively. At each height, the profiles are reported at quarter cycle intervals (when $T_h = \bar{T}_{h,max}$; $T_h = \bar{T}_{h,min}$ and $T_h = \bar{T}_h$ increasing and $T_h = \bar{T}_h$ decreasing) over the duration of the fourth cycle.

Referring to the temperature profiles, it is immediately apparent that the oscillating hot wall temperature variation is felt only partially in the enclosure. The depth of penetration increases with the enclosure height. For example, at $y = 0.07$ (Fig. 7(d)), the hot wall temperature variation extends to $x \simeq 0.1$ whereas at $y = 0.93$ the temperature variation penetrates to $x \simeq 0.42$ (Fig. 7(a)). Past these points the temperature profiles (hence the heat flux) become time-independent. Finally, note that the presence of the 'backward' heat flow in the top half of the enclosure is indicated by the positive slope of the temperature profiles at the hot wall shown at two of the four times reported in Figs. 7(a) and (b).

The velocity profiles plotted in Fig. 7 reveal that the vertical velocity component near the cold wall remains virtually unchanged over time but deviates greatly as the hot wall is approached. This shows that higher velocities are associated with higher hot wall temperatures.

Effect of amplitude

Simulations 2 and 3 (Table 1) were performed to determine the effect that the amplitude of the temperature oscillation has on the system behavior. The parameters used in runs 1–3 were all identical except for the amplitude, which varied four-fold from $a = 0.2$ (simulation 2) to $a = 0.8$ (simulation 3). The amplitude of the first run was set at $a = 0.4$, exactly halfway between the two extremes. The results of this first simulation were thoroughly discussed earlier in terms of the basic physics involved in this problem and serve as a foundation for further discussion.

For brevity we will discuss the results of simulations 2 and 3 together and will focus only on those aspects that significantly change with amplitude. The streamline and isotherm plots for runs 2 and 3 are shown in Figs. 8 and 9, respectively. The amplitude of the hot wall temperature was $a = 0.2$ in run 2 and $a = 0.8$ in run 3. For both cases, the solution became periodic after just two cycles. The contours shown in Figs. 8 and 9 are the results plotted quarterly during the fourth cycle of the simulations. Generally speaking, we find that the same basic fluid flow and heat transfer phenomenon identified earlier in connection with the first simulation still applies both when we decrease (Fig. 8) or increase (Fig. 9) the hot wall temperature amplitude. However, the region of secondary recirculation and the region of back heat flow differ greatly in size and magnitude. When $a = 0.2$, the secondary cell is very small (Fig. 8(d)) and appears only for a short time. On the other hand, for $a = 0.8$, the secondary cell is much larger, greater in intensity, and

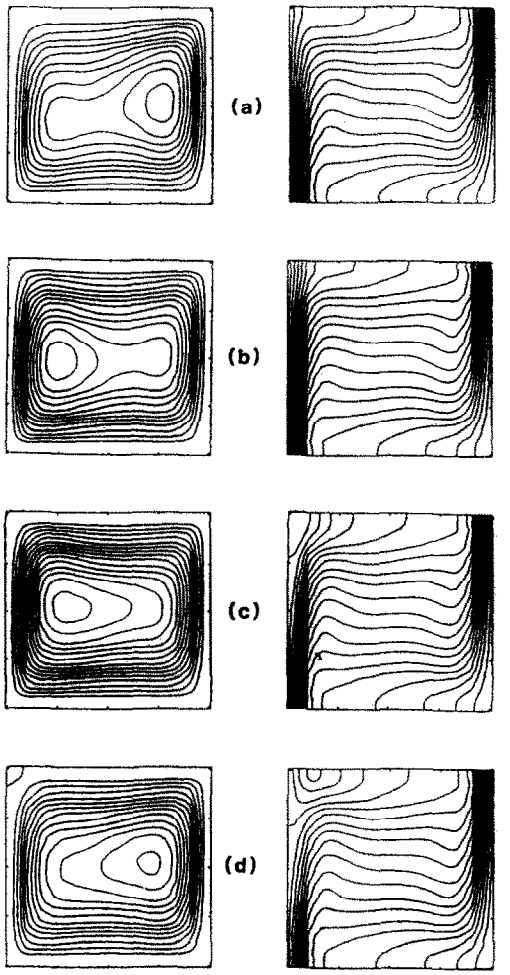

FIG. 8. Periodic streamlines (left column) and isotherms (right column) for simulation 2. (a) $\tau = 0.03$, $\psi_{max} = 11$. (b) $\tau = 0.0325$, $\psi_{max} = 13$. (c) $\tau = 0.0350$, $\psi_{max} = 15$. (d) $\tau = 0.0375$, $\psi_{max} = 13$. Streamlines increment $\Delta\psi = 1.0$ for primary cell and $\Delta\psi = -1.0$ for secondary cell. Isotherms increment $\Delta\theta = 0.05$ starting at $\theta = 0$ from the right.

exists for a longer duration of time (Figs. 9(a)–(d)). The location of ψ_{max} in the primary cells shifts from side-to-side in a similar fashion for both amplitudes, but the maximum magnitude changes more with time at the higher amplitude, i.e. $7 \leqslant \psi_{max} \leqslant 22$ for $a = 0.8$ whereas $11 \leqslant \psi_{max} \leqslant 15$ at $a = 0.2$. Comparing runs 2 and 3 further it is observed that back heat flow occurs only over 25% of the hot wall surface for $a = 0.2$ (Fig. 8(d)). By contrast, it extends over the entire hot wall surface when $a = 0.8$ (Fig. 9(d)). This fact is reflected in the Nusselt number versus time plots shown in Fig. 10. When the hot wall variation is small ($a = 0.2$), the hot wall Nusselt number remains positive for all times (Fig. 10(a)). However, when the system is subjected to a much higher temperature variation ($a = 0.8$), the Nusselt number evaluated at the hot wall becomes negative (Fig. 10(b)) over a fairly large portion of the cycle. Of importance is the

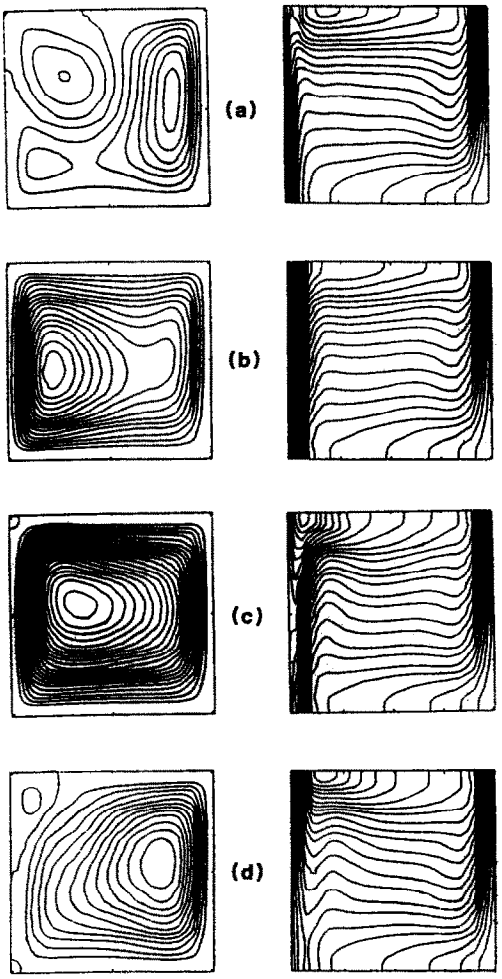

FIG. 9. Periodic streamlines (left column) and isotherms (right column) for simulation 3. (a) $\tau = 0.03$, $\psi_{max} = 7$. (b) $\tau = 0.0325$, $\psi_{max} = 16$. (c) $\tau = 0.0350$, $\psi_{max} = 22$. (d) $\tau = 0.0375$, $\psi_{max} = 12$. Streamline increment $\Delta\psi = 1.0$ for primary cell and $\Delta\psi = -1.0$ for secondary cell. Isotherms increment $\Delta\theta = 0.05$ starting at $\theta = 0$ from the right.

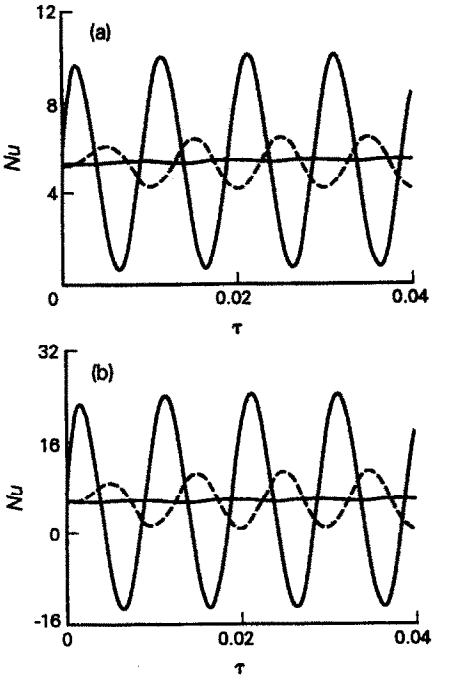

FIG. 10. Nusselt number dependence on time. Hot wall, $x = 0$ (——); cold wall, $x = L/H$ (— · —); midpoint, $x = (L/2)/H$ (— —). (a) Simulation 2. (b) Simulation 3.

fact that the Nusselt numbers, for both amplitudes, become constant at the cold wall and roughly equal the same value.

Effect of period

The last two runs listed in Table 1 examine the dependence of the system behavior on the period at which the hot wall temperature oscillates. The hot wall temperature varied exactly by the same amount ($a = 0.4$) in simulations 4 and 5 but took four times longer to change in run 5 ($p = 0.02$) as compared to run 4 ($p = 0.005$).

The first major difference detected between these two runs was the number of cycles required for the solution to become periodic. The solution repeated itself immediately after the first cycle when the wall changed at a slow rate (run 5), while it took more than four cycles to become periodic when the hot wall temperature changed much faster (run 4). Recall that the initial transient died after two cycles in simulation 1 (the same amplitude as runs 4 and 5 but with a period halfway between the two extremes).

Once periodic, the differences in the flow and temperature fields are determined by comparing Fig. 11 (run 4, $p = 0.005$) to Fig. 12 (run 5, $p = 0.02$). Both sequences shown in Figs. 11 and 12 report the periodic solution at quarterly time intervals starting at $T_h = \bar{T}_h$ and increasing. At first glance, the contours show the same basic process for both cases as described in the earlier runs, but a close inspection, however, reveals several important differences. First, the size and the magnitude of the secondary cell is larger when the system has a longer period of temperature oscillation. Second, the extent of back heat flow depends on the period and is larger for the system with the shorter period. Comparing the isotherms in Fig. 11(d) to the isotherms in Fig. 12(d) shows that back heat flow occurs over 25% more surface area at the shorter period. Ramping the wall temperature at a slower rate allows more time for the system to respond and reduces back heat flow.

It is also observed that the longer the time period of oscillation, the greater the fluctuation in the maximum stream function. The system with the greater time period has a large variation in ψ_{max}, $10 \leqslant \psi_{max} \leqslant 18$ (Fig. 12), while ψ_{max} is almost constant, $12 \leqslant \psi_{max} \leqslant 14$, for the system with a short time period (Fig.

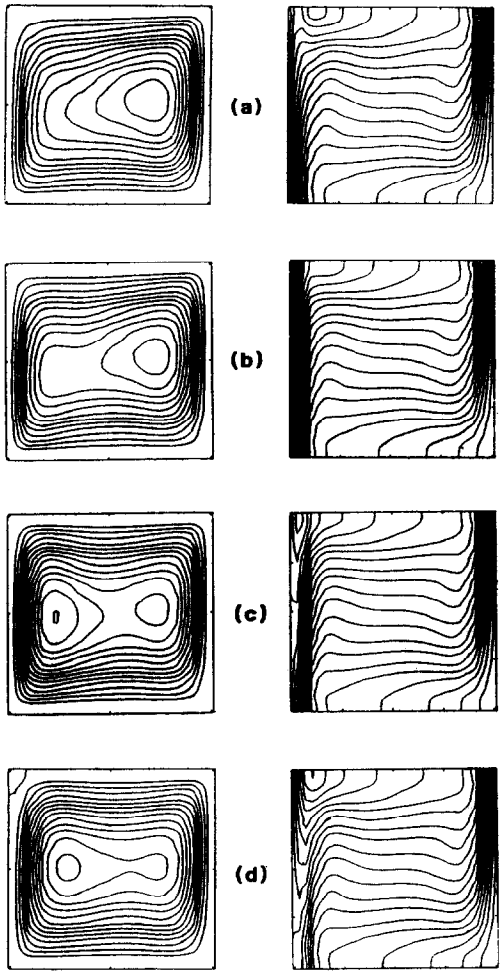

FIG. 11. Periodic streamlines (left column) and isotherms (right column) for simulation 4. (a) $\tau = 0.015$, $\psi_{max} = 12$. (b) $\tau = 0.01625$, $\psi_{max} = 12$. (c) $\tau = 0.0175$, $\psi_{max} = 14$. (d) $\tau = 0.01875$, $\psi_{max} = 13$. Streamline increment $\Delta\psi = 1.0$ for primary cell and $\Delta\psi = -1.0$ for secondary cell. Isotherms increment $\Delta\theta = 0.05$ starting at $\theta = 0$ from the right.

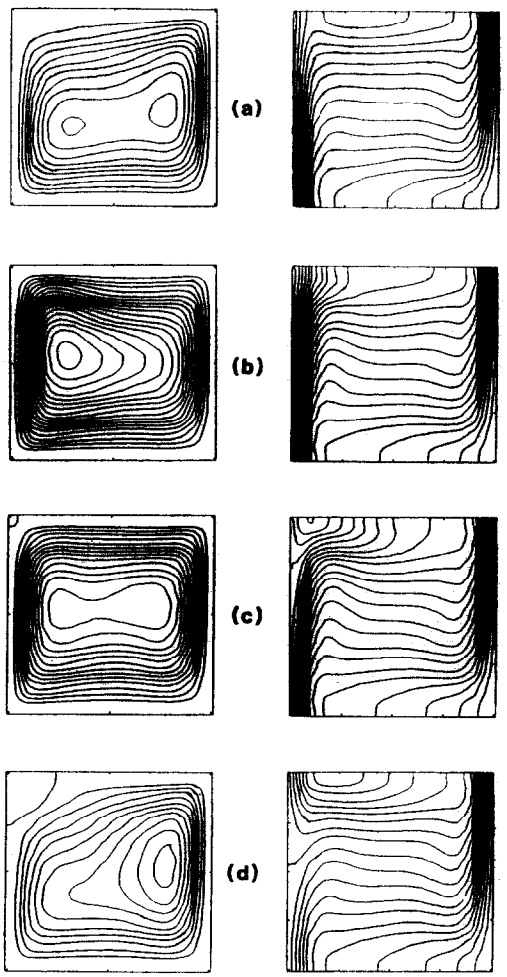

FIG. 12. Periodic streamlines (left column) and isotherms (right column) for simulation 5. (a) $\tau = 0.06$, $\psi_{max} = 10$. (b) $\tau = 0.065$, $\psi_{max} = 18$. (c) $\tau = 0.07$, $\psi_{max} = 13$. (d) $\tau = 0.075$, $\psi_{max} = 10$. Streamline increment $\Delta\psi = 1.0$ for primary cell and $\Delta\psi = -1.0$ for secondary cell. Isotherms increment $\Delta\theta = 0.05$ starting at $\theta = 0$ from the right.

11). The location of the maximum stream function is in phase with the hot wall boundary condition when the wall changes at a slow rate (Fig. 12) but lags by at least 90° for the shorter time period case (Fig. 11).

The degree of penetration of the time-dependent boundary condition into the enclosure strongly depends on the period of oscillation. Shorter periods show less penetration, and longer periods result in greater depth of penetration. This is the same trend that is found in pure conduction heat transfer with an oscillating boundary condition [13]. This conclusion is drawn in this study by comparing the isotherms in Fig. 11 to the isotherms in Fig. 12 at equivalent times. A careful comparison of the isotherm patterns shows that the change occurring near the hot wall, with respect to time, is restricted to a thinner region for the simulation with the shorter time period. This fact is also evident in Figs. 13(a), (b), which shows the Nusselt number fluctuation diminishing more quickly with distance for short time periods (Fig. 13(a)) than for long time periods (Fig. 13(b)).

Time-averaged heat transfer

The last issue to address is that of heat transfer enhancement caused by wall temperature oscillation. To answer this question, consider the time-averaged heat transfer

$$\overline{Nu} = \frac{1}{p}\int_{\text{cycle}} Nu\,\mathrm{d}\tau. \tag{10}$$

The instantaneous Nusselt number, Nu, was defined earlier in equation (9) as the dimensionless heat transfer across a vertical cross-section at a particular instant. Integration over a complete cycle yields the time-averaged value. Once the solution becomes

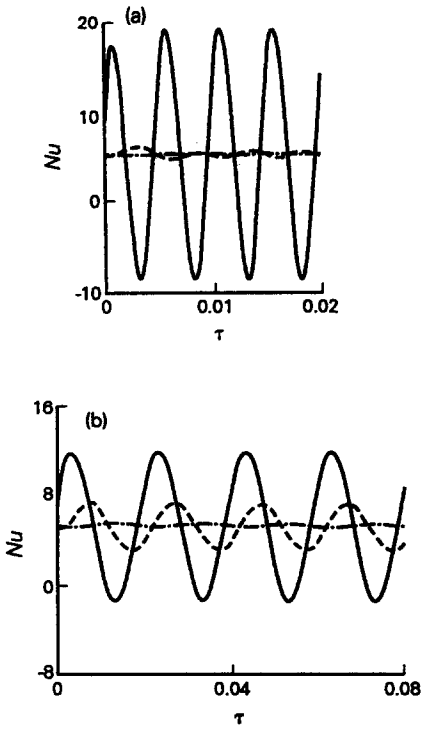

FIG. 13. Nusselt number dependence on time. Hot wall, $x = 0$ (——); cold wall, $x = L/H$ (—·—); midpoint, $x = (L/2)/H$ (– – –). (a) Simulation 4. (b) Simulation 5.

periodic, $\overline{Nu}$ becomes constant and independent of the location of X (i.e. $\overline{Nu}_c = \overline{Nu}_h = \overline{Nu}_{L/2}$). Values of Nu are reported in Table 2 for all of the simulations along with the percentage increase (shown in parentheses) above the constant wall temperature solution.

Results of our study (Table 2) show that the time-averaged heat transfer increases only marginally due to the hot wall temperature oscillation. Two trends are easily identified in Table 2. Increasing the amplitude (for fixed period) or increasing the period (for fixed amplitude) slightly increases the time-averaged heat transfer. Note also that higher amplitudes and longer periods mean more penetration of the temperature oscillation into the cavity. Since the temperature oscillation does not fully penetrate to the opposite cold vertical wall, it is not surprising that the increase in the time-averaged heat transfer through the enclosure is small.

Table 2. Periodic time-averaged Nusselt number

Simulation number	a	P	$\overline{Nu}$
1	0.4	0.01	5.41 (1.7%)
2	0.2	0.01	5.35 (0.6%)
3	0.8	0.01	5.58 (4.9%)
4	0.4	0.005	5.36 (0.8%)
5	0.4	0.02	5.43 (2.1%)

CONCLUSIONS

This study helped clarify the role and relative importance of time-dependent boundary conditions on thermally-driven convection in enclosures. More specifically, this paper numerically investigated natural convection in a square enclosure with an oscillatory hot wall temperature opposite a vertical constant cold wall. For the parametric domain investigated, the following main conclusions were reached.

(1) The solution became periodic after a small number of cycles. The number depended inversely on the period but was independent of the amplitude.

(2) The periodic flow field in all cases consisted of a primary cell which fluctuated in intensity and in the location of ψ_{max}. A weak secondary cell periodically appeared in the upper left hand corner of the enclosure and back heat flow occurred over certain times over a large portion of the hot driving wall. The wall temperature oscillations penetrated only partially into the enclosure. The Nusselt number varied with the same period as the hot wall temperature. Its amplitude quickly decreased with distance into the enclosure and became nearly constant at the cold wall.

(3) Increasing the amplitude or the period of the hot wall temperature oscillation increased the size and the intensity of the secondary region of recirculation and increased the distance the hot wall temperature variation was felt into the enclosure. Also, greater variation in ψ_{max} is associated with larger values of amplitude and longer periods.

(4) Increasing the amplitude or decreasing the period of the hot wall temperature oscillation increased the extent and the duration of the back heat flow.

(5) Despite the time-dependent boundary condition and the drastically changing flow and temperature fields, the *average* heat transfer across the enclosure per cycle was approximately equal to the value for the enclosure with a fixed (mean) hot wall temperature. Increasing the amplitude or the period of the hot wall temperature oscillation increased the cycle-averaged heat transfer only slightly.

Acknowledgements—This work was supported in part through grant 2-07044 from UARC. The first author also acknowledges useful discussions held with Professor D. Poulikakos of the University of Illinois at Chicago.

REFERENCES

1. K. T. Yang, Natural convection in enclosures. In *Handbook of Single-phase Convective Heat Transfer* (Edited by S. Kakac, R. Shah and W. Aung), Chap. 13. Wiley, New York (1987).
2. J. Patterson and J. Imberger, Unsteady natural convection in a rectangular cavity, *J. Fluid Mech.* **100,** 65–86 (1980).
3. K. Kublbeck, G. P. Merker and J. Straub, Advanced numerical computation of two-dimensional time-dependent free convection in cavities, *Int. J. Heat Mass Transfer* **23,** 203–217 (1980).
4. G. N. Ivey, Experiments on transient natural convection in a cavity, *J. Fluid Mech.* **144,** 389–401 (1984).

5. S. G. Schladow, J. C. Patterson and R. L. Street, Transient flow in a side-heated cavity at high Rayleigh number: a numerical study, *J. Fluid Mech.* **200,** 121–148 (1989).
6. J. M. Hyun and J. W. Lee, Numerical solutions for transient natural convection in a square cavity with different sidewall temperatures, *Int. J. Heat Fluid Flow* **10,** 146–151 (1989).
7. V. F. Nicolette, K. T. Yang and J. R. Lloyd, Transient cooling by natural convection in a two-dimensional square enclosure, *Int. J. Heat Mass Transfer* **28,** 1721–1732 (1985).
8. J. D. Hall, A. Bejan and J. B. Chaddock, Transient natural convection in a rectangular enclosure with one heated side wall, *Int. J. Heat Fluid Flow* **9,** 396–404 (1988).
9. P. Vasseur and L. Robillard, Natural convection in a rectangular cavity with wall temperature decreasing at a uniform rate, *Wärme- und Stoffübertr.* **16,** 199–207 (1982).
10. S. V. Patankar, *Numerical Heat Transfer and Fluid Flow*, p. 90. McGraw-Hill, New York (1980).
11. D. A. Anderson, J. C. Tannehill and R. H. Pletcher, *Computational Fluid Mechanics and Heat Transfer*, p. 507. McGraw-Hill, New York (1984).
12. M. J. Kazmierczak, Transient double diffusion in a fluid layer and in a composite porous-fluid layer heated from below, Ph.D. Thesis, University of Illinois at Chicago, Chicago, Illinois (1988).
13. G. E. Myers, *Analytical Methods in Conduction Heat Transfer*, Chap. 5. McGraw-Hill, New York (1971).

ECOULEMENT DE CONVECTION NATURELLE DANS UNE CAVITE AVEC DES CONDITIONS AUX LIMITES PERIODIQUES DANS LE TEMPS

Résumé—On étudie numériquement le problème de l'écoulement laminaire de convection naturelle dans une cavité carrée ayant une paroi verticale chaude à température uniforme mais périodiquement variable dans le temps. Cette température varie sinusoïdalement autour d'une température fixée. La paroi opposée froide est maintenue à température constante. Des solutions sont obtenues pour différents cas qui illustrent les effets des oscillations de température de la surface sur l'écoulement et le transfert thermique à travers la cavité. Les solutions obtenues sont périodiques dans le temps. Ces lignes de courant montrent qu'un petit écoulement secondaire apparaît de façon intermittente dans le coin supérieur près de la paroi chaude et qu'il tourne dans le sens opposé à celui de l'écoulement principal. Le flux thermique instantané à travers la surface fluctue fortement et pendant une certaine durée, la chaleur enlevée concerne un large segment de la surface chaude. L'effet du changement périodique de température pariétale est partiellement sensible dans la cavité et globalement le transfert moyenné dans le temps, à travers la cavité, est pratiquement insensible à la condition thermique périodique.

AUFTRIEBSSTRÖMUNG IN EINEM HOHLRAUM MIT ZEITLICH PERIODISCHEN RANDBEDINGUNGEN

Zusammenfassung—Das Problem der laminaren Auftriebsströmung in einem quadratischen Hohlraum wird numerisch untersucht. Die Strömung entsteht dadurch, daß eine senkrechte Wand eine gleichförmige, zeitlich periodisch schwankende Oberflächentemperatur besitzt. Die Temperaturschwankungen sind sinusförmig, ihr Mittelwert konstant. Die gegenüberliegende kalte Wand wird auf konstanter Temperatur gehalten. Für eine Anzahl unterschiedlicher Fälle werden Lösungen ermittelt, die die Einflüsse der oszillierenden Oberflächentemperatur auf die Fluidströmung und den Wärmeübergang im Hohlraum aufzeigen. Die ermittelten transienten Lösungen sind alle zeitlich periodisch. Die Stromlinien zeigen eine schwache sekundäre Strömungszelle, die intermittierend auftritt und anschließend in der oberen Ecke des Hohlraums nahe der wärmeren Wand verschwindet. Diese Zellen rotieren umgekehrt zur Hauptströmung. Der Momentanwert der Wärmestromdichte durch die heiße Wand weist starke zeitliche Schwankungen auf, wobei es in bestimmten Zeitintervallen zur Rückströmung von Wärme in großen Teilen der heißen Fläche kommt. Der Einfluß der periodisch schwankenden Wandtemperatur ist nur teilweise im Hohlraum festzustellen. Im ganzen gesehen ist der zeitlich gemittelte Wärmeübergang im gesamten Hohlraum ziemlich unempfindlich gegenüber der zeitabhängigen Randbedingung.

ВЫЗВАННОЕ ПОДЪЕМНОЙ СИЛОЙ ТЕЧЕНИЕ В ПОЛОСТИ С ПЕРИОДИЧЕСКИ ИЗМЕНЯЮЩИМИСЯ ВО ВРЕМЕНИ ГРАНИЧНЫМИ УСЛОВИЯМИ

Аннотация—Численно исследуется задача о вызванном подъемной силой ламинарнсм течении в квадратной полости с нагретой вертикальной стенкой, на поверхности которой поддерживается одинаковая температура, периодически изменяющаяся во времени. Эта температура изменяется синусоидально, колеблясь около фиксированного среднего значения. Противоположная ненагретая стенка поддерживается при постоянной температуре. Получены решения для ряда случаев, иллюстрирующие влияние колебаний температуры поверхности на течение жидкости и теплоперенос в полости. Все полученные нестационарные решения периодически изменяются во времени. Линии тока свидетельствуют о том, что в верхнем углу полости у нагретой стенки периодически возникает и затем исчезает ячейка слабого вторичного течения, вращающаяся в направлении, обратном основному течению. Мгновенный теплоперенос через нагретую стенку существенно фуктуирует во времени и спустя некоторое время происходит отвод тепла с большого участка нагретой поверхности. Эффект периодического изменения температуры стенки проявляется в полости лишь частичо, и в целом осредненный по времени теплоперенос мало зависит от нестационарных граничных условий.